Electronic Supplementary Material (ESI)

Direct Z-Scheme Cs_2O-Bi_2O_3-ZnO Heterostructures for Photocatalytic Overall Water Splitting

Abdo Hezam,[a] K. Namratha,[a] Q.A. Drmosh,[b] Deepalekshmi Ponnamma,[c] Adel Morshed Nagi Saeed,[d] V.Ganesh,[e] B. Neppolian,[f] and K.Byrappa *[a]

[a] Center for Materials Science and Technology, University of Mysore, Vijana Bhavana, Manasagangothiri, Mysuru-570006, India.

[b] Physics Department and Center of Research Excellence in Nanotechnology, King Fahd University of Petroleum and Minerals, Dhahran 31261, Saudi Arabia.

[c] Center for Advanced Materials, Qatar University, P O Box 2713, Doha, Qatar

[d] Department of Polymer Science and Technology, Sri Jayachamarajendra College of Engineering, JSS Science & Technology University, Mysuru – 570 006, India.

[e] Department of Physics & Nanotechnology, SRM Institute of Science and Technology, Chennai-603203, India.

[f] Energy and Environmental Remediation Lab, SRM-Research Institute, SRM Institute of Science and Technology, Chennai-603203, India.

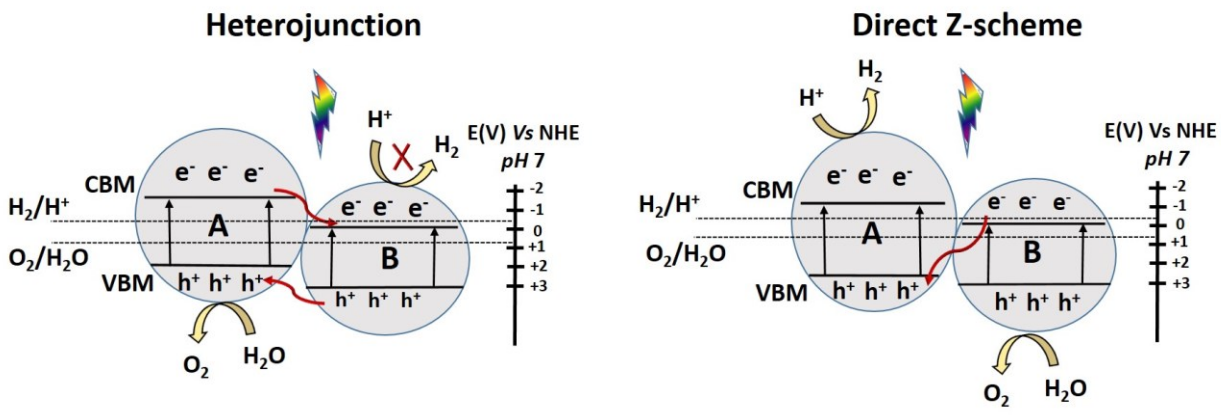

Scheme S1. Comparison of charge carriers migration pathway in heterojunction and direct Z-scheme systems.

PXRD studies

Figure S1 shows comparison between the PXRD patterns of Cs_2O-Bi_2O_3-ZnO (samples CBZ0.5, CBZ1, CBZ1.5 and CBZ2), Bi_2O_3-ZnO heterostructures (sample CBZ0), pristine Bi_2O_3, pristine ZnO, and pristine Cs_2O. The PXRD patterns of Bi_2O_3, ZnO, and Cs_2O are well matched with JCPDS file no. 71-2274, JCPDS Card No. 36-1451, and JCPDS file no. 71-2274, respectively, indicating the monoclinic crystal structure of Bi_2O_3 and the hexagonal structure of ZnO and Cs_2O. The Cs_2O-Bi_2O_3-ZnO heterostructure consists of three phases namely, hexagonal Cs_2O (PDF #09-0104) [1], hexagonal ZnO (JCPDS Card No. 36-1451) [2] and monoclinic α-Bi_2O_3 (JCPDS file no. 71-2274) [3] while the PXRD pattern of the sample CBZ0 reveals that the Bi_2O_3-ZnO consists of monoclinic α-Bi_2O_3 and hexagonal ZnO phases only. Moreover, the PXRD study indicates that no crystal impurities are detected confirming the purity of the prepared heterostructures..

The characteristics peaks of Cs_2O appear on the spectrum of CBZ1.5 at 2θ= 18.2, 25.7, and 42.51° (JCPDS 09-0104). The peaks at 31.69, 34.83, and 36.16° for both CBZ1.5 and CBZ0 samples correspond to the hexagonal phases of ZnO (JCPDS 36-1451). The remaining peaks observed are due to the monoclinic phase of α-Bi_2O_3 (JCPDS 71-2274). It is worth noting that the peak intensity and/or peak width of heterostructures are not similar to those of pristine metal oxides indicating a change in the crystal growth and the size of heterostructure nanoparticles and confirming the formation of nanoscale heterostructures [4,5]. These results confirm the successful formation of Cs_2O-Bi_2O_3-ZnO and Bi_2O_3-ZnO heterostructures.

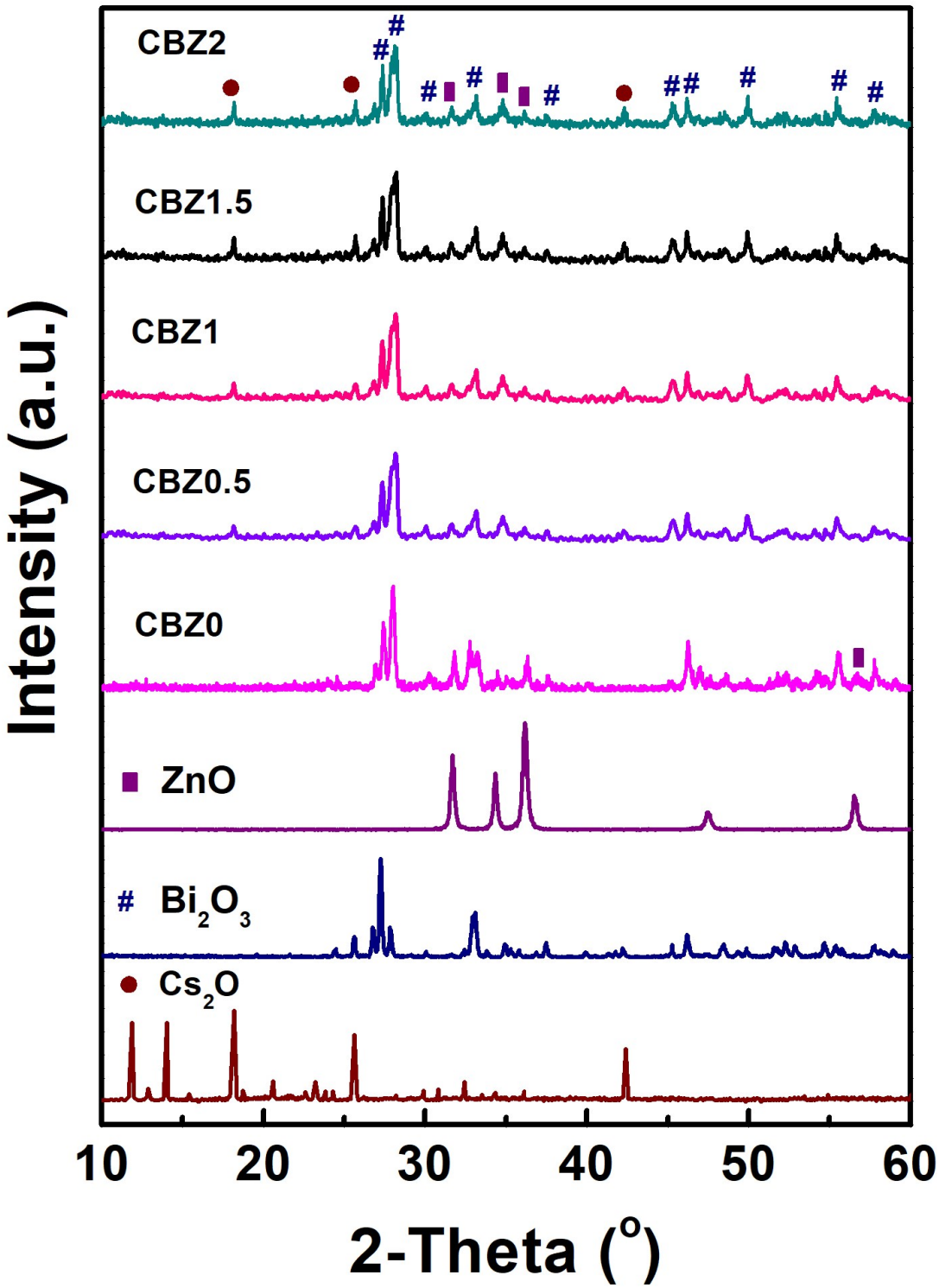

Fig. S1. PXRD patterns of Cs_2O, Bi_2O_3, ZnO, CBZ0, CBZ0.5, CBZ1, CBZ1.5, and CBZ2 samples.

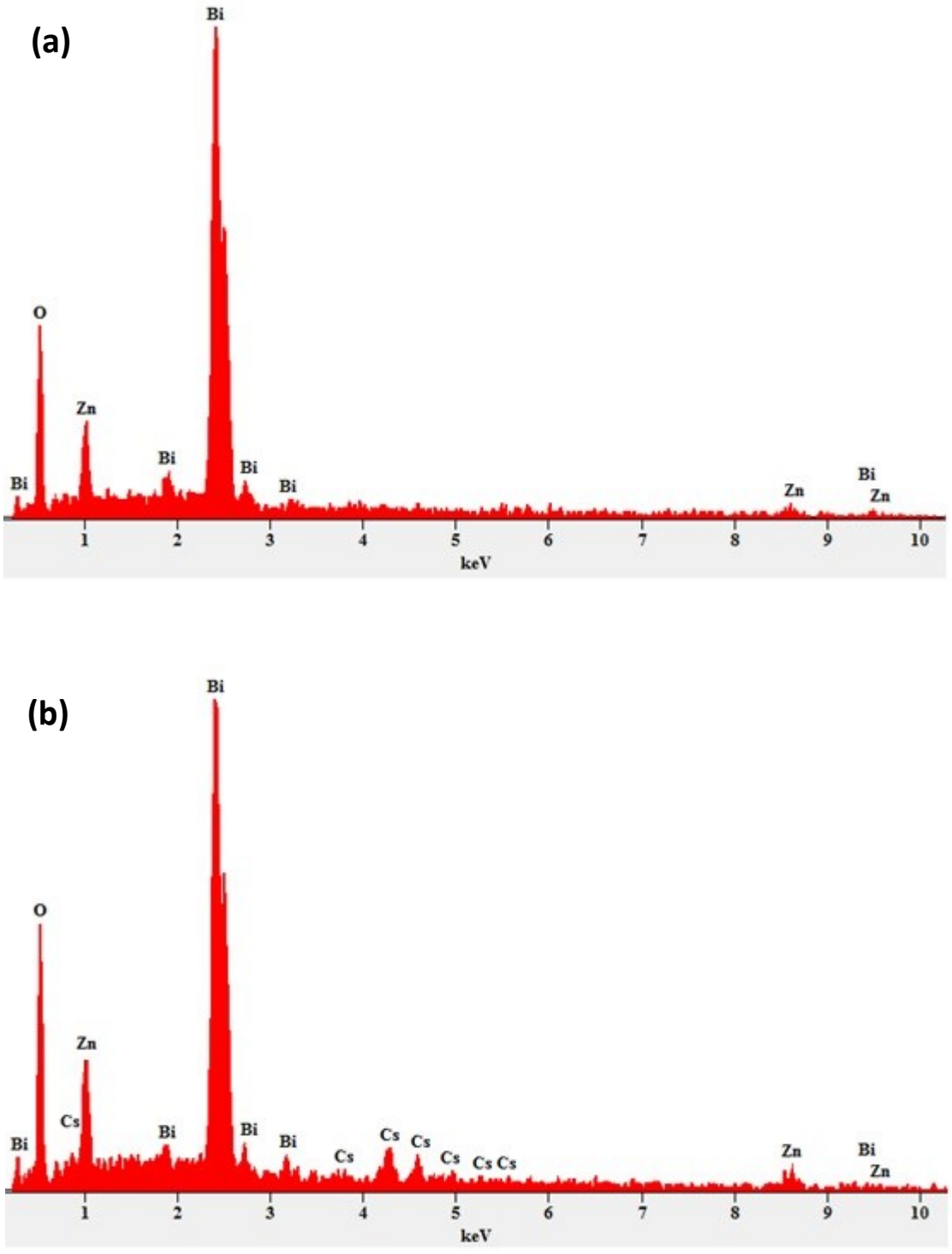

Fig. S2. EDX spectra of (a) Bi_2O_3-ZnO heterostucture (sample CBZ0), and (b) the optimized Cs_2O-Bi_2O_3-ZnO heterostucture (sample CBZ1.5).

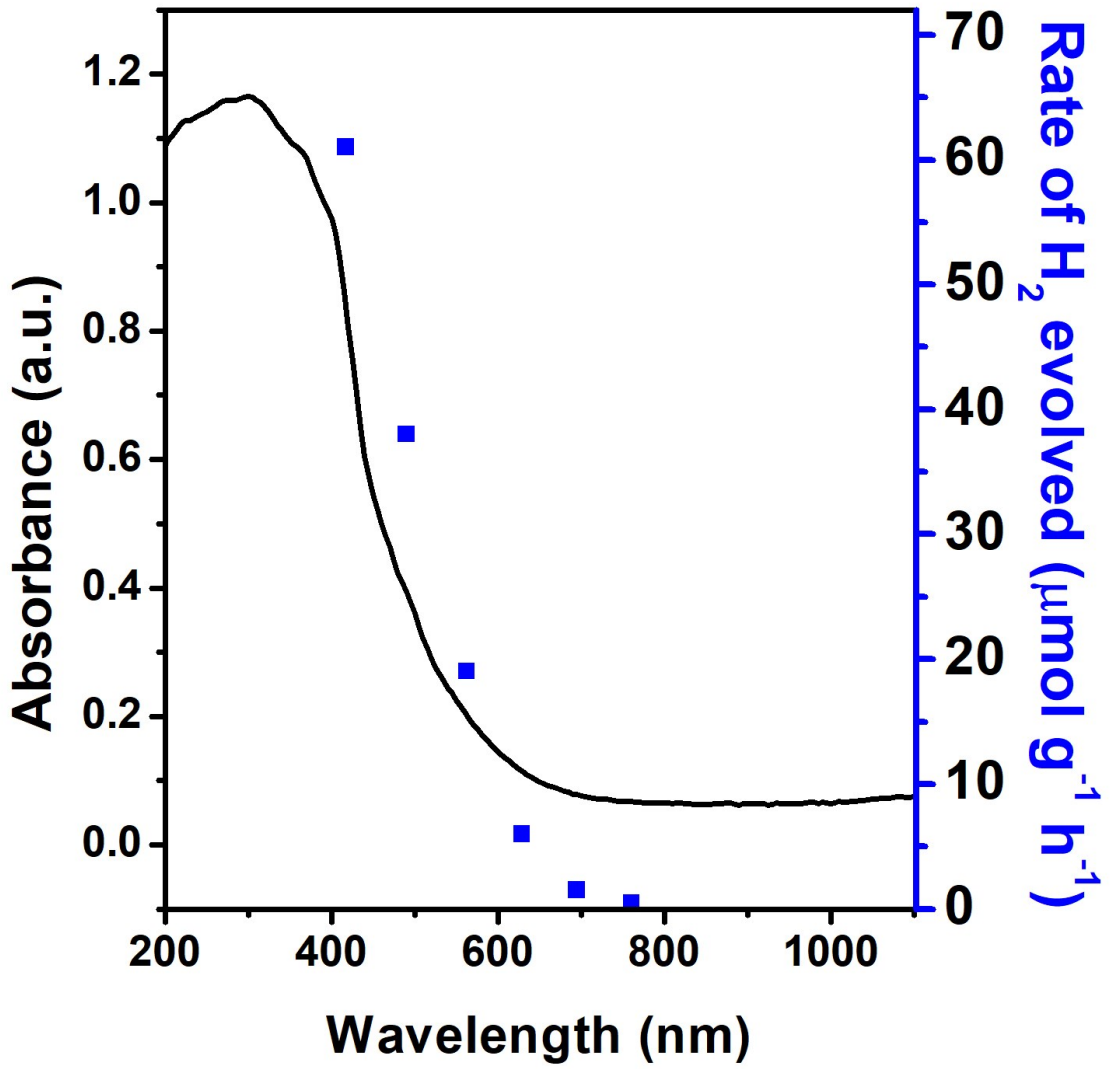

Fig. S3. Dependence of the rate of H_2 evolved on the wavelength of incident light (blue line) and the DRS UV-vis of CBZ1.5 sample (black line). Reaction conditions: 5 m g CBZ1.5 ; pure water; simulated sunlight (AM 1.5 G,).

Fig. S3 shows that the positive relation between the photocatalytic activity of Cs_2O-Bi_2O_3-ZnO and its optical absorption property (Fig. 5b).

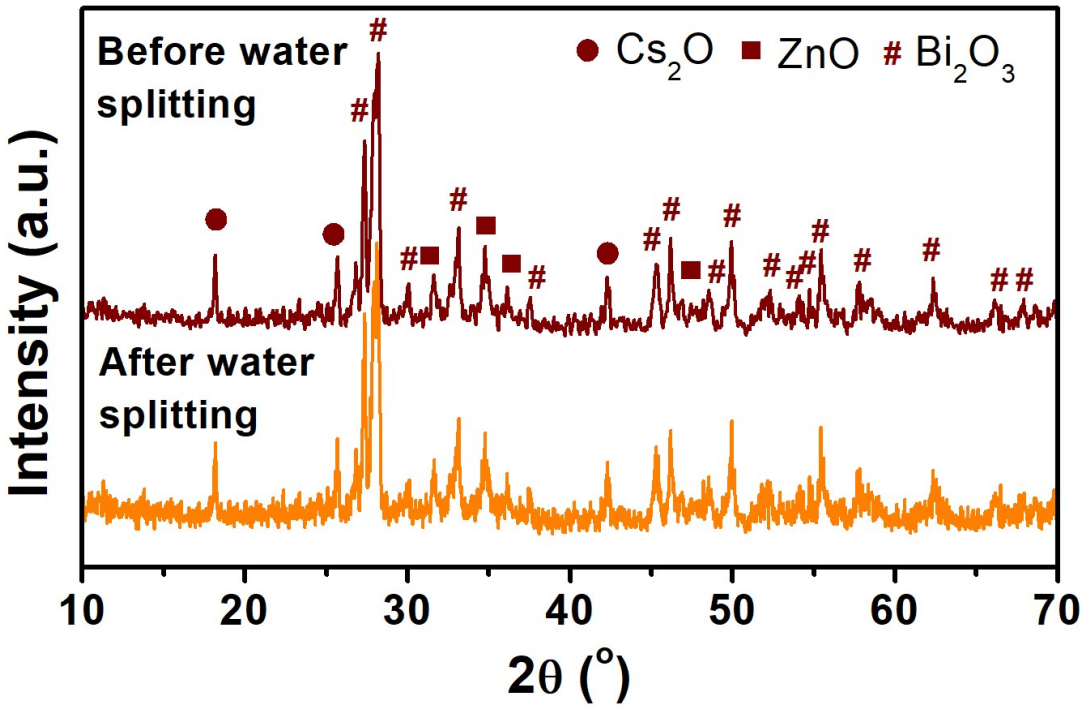

Fig. S4. PXRD patterns of the sample CBZ1.5 before and after water splitting experiment.

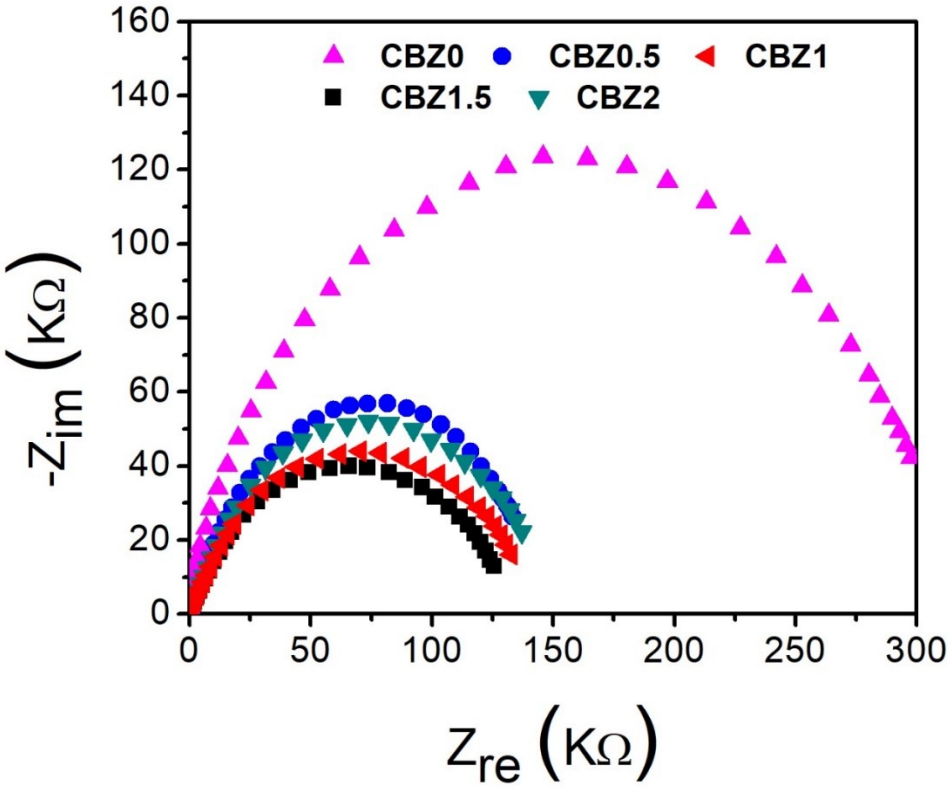

Fig. S5. Nyquist impedance plots of the different prepared samples.

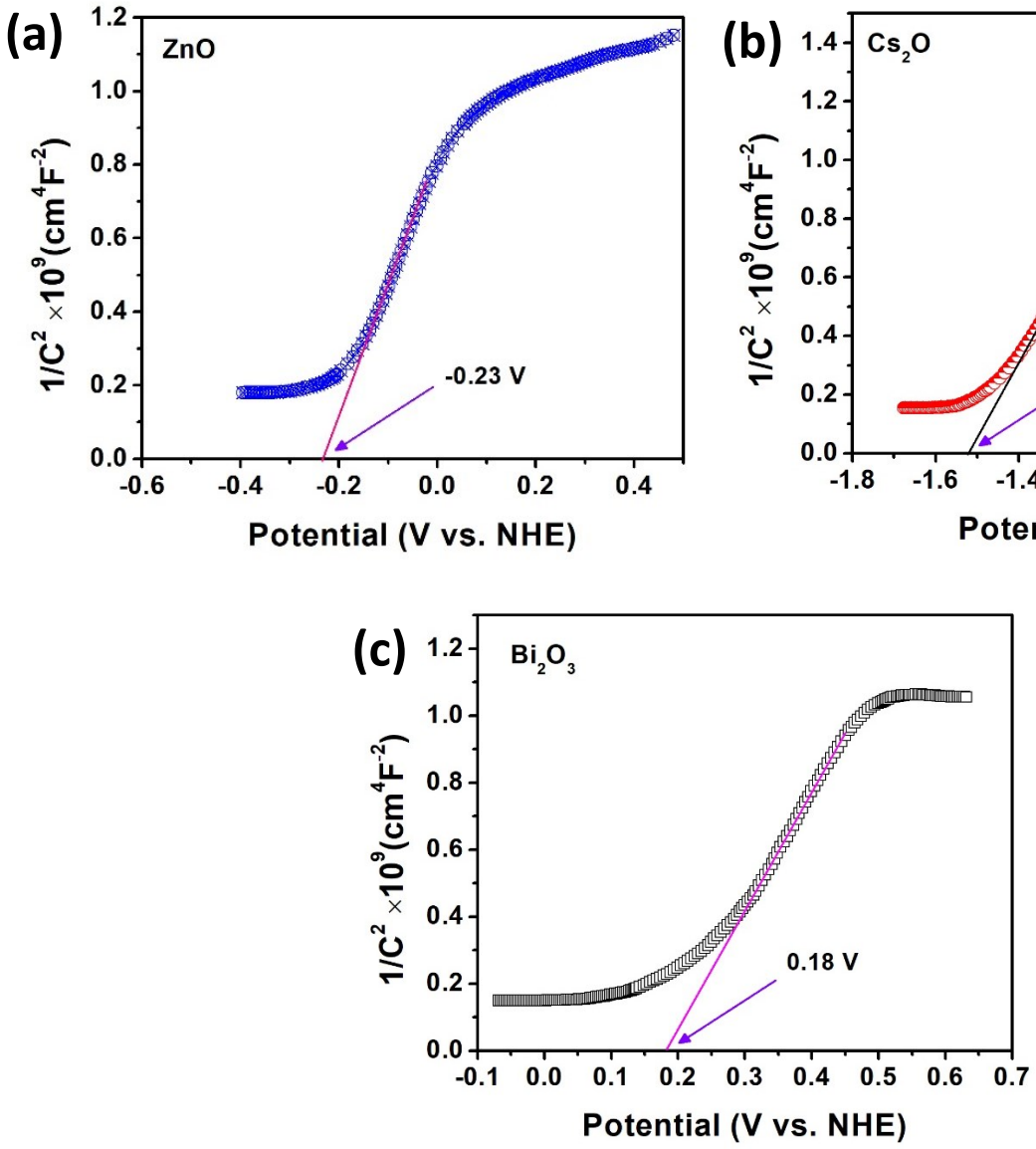

Fig. S6 Mott-Schottky plots for pristine (a) ZnO, (b) Cs_2O, and (c) Bi_2O_3.

The photocatalytic water splitting of Cs_2O under simulated sunlight irradiation (AM 1.5 G) in the absence of sacrificial agents (pure water) and in the presence of methanol and glycerol was measured and the results were presented in Figure S7. No H_2 molecules were detected in the absence of sacrificial agents. However, hydrogen production was 232 $\mu molg^{-1}h^{-1}$ in the presence of methanol (50% (v/v) methanol/water) and 556 $\mu molg^{-1}h^{-1}$ in the presence of glycerol (25% (v/v) glycerol/water). The higher hydrogen production rate in the presence of glycerol than methanol is attributed to higher polarity of glycerol.[6] CBM of Cs_2O (-1.55 eV) is suitable to produce H_2 but it VBM (0.41 eV) is not suitable to produce O_2, therefore, Cs_2O was unable to split pure water in the absence of sacrificial agents. Sacrificial agents react with holes to reduce the electron-hole recombination and increase the photocatalytic activity of Cs_2O.

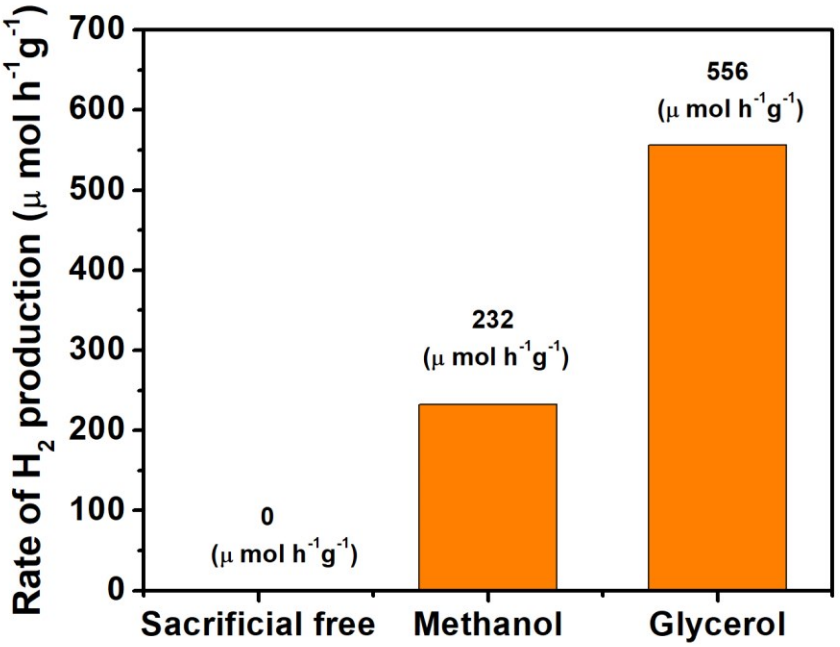

Fig. S7 Photocatalytic hydrogen production activity of pure Cs_2O in the absence of sacrificial agents and in the presence of methanol and glycerol under simulated sunlight irradiation (AM 1.5 G).

To further explore the impact of Cs_2O, the photocatalytic hydrogen production experiment was repeated using Bi_2O_3-ZnO as a photocatalyst in the presence of different sacrificial agents including methanol, glycerol, and triethanolamine (TEOA) solution. No H_2 was detected in each experiment. The formation of a junction between Bi_2O_3 and ZnO makes Bi_2O_3-ZnO unable to produce H_2 even after adding sacrificial agents. This happens as the electrons are accumulated in the CB of Bi_2O_3 which is more positive compared to H^+/H_2. Thus, Cs_2O played a significant role in enhancing the photocatalytic activity of Cs_2O-Bi_2O_3-ZnO heterostructure through constructing a Z-scheme system with Bi_2O_3 and ZnO and extending its light absorption range.

Table S1. Elemental analysis of Bi_2O_3-ZnO and Cs_2O-Bi_2O_3-ZnO heterostructures

Sample	**Bi**	**Zn**	**Cs**	**O**	**Total**	**Bi:Zn**
CBZ0 (Bi_2O_3-ZnO)	25.39 atom %	17.82 atom %	0 atom %	56.79 atom %	100 atom %	1:0.702
CBZ1.5 (Cs_2O-Bi_2O_3-ZnO)	21.78 atom %	15.32 atom %	0.67 atom %	62.23 atom %	100 atom %	1:0.703

Table S2. Overall water splitting using different samples under simulated sunlight irradiation Am 1.5 G.

Sample	H_2 (μmol h^{-1} g^{-1})	O_2 (μmol h^{-1} g^{-1})
CBZ0	0	0
CBZ0.5	65.2	31.9
CBZ1	123.9	62.1
CBZ1.5	149.5	73.2
CBZ2	97.8	47.7

Table S3. Summary of the recent Z-scheme photocatalysts for overall water splitting.

	Z-scheme systems with co-catalyst and or electrons mediator for Overall water splitting						
Entry	**Photocatalyst**	**AQE**	**Activity**	**Conditions of photocatalytic reaction**	**Electrons Mediator**	**Co-Catalyst**	**Ref**
1	$MgTa_2O_{6-x}N_y$/TaON/PtO_x-WO_3	6.8% at 420 nm	H_2: 480 μmol h^{-1} g^{-1} O_2: 250 μmol h^{-1} g^{-1}	λ> 420 nm (Xenon lamp, 300 W) $9.1x10^{21}$ photon h^{-1}	Yes	Yes	***Angew. Chem***. Int. Ed. 2015, 54, 8498 –8501
2	$SrTiO_3$:La,Rh/Au/$BiVO_4$	5.9% at 418 nm	H_2: 2100 μmol h^{-1} g-1 O_2: 1000 μmol h^{-1} g^{-1}	λ> 420 nm (Xenon lamp, 300 W)	Yes	Yes	***J. Catal.*** 2015, 328, 308–315
3	$RhCrO_x$/ZrO2/$LaMg_{1/3}Ta_{2/3}O_2N$)/ Au/$BiVO_4$:Mo	0.07% at 418 nm	H_2: 60 μmol h-1 g-1 O_2: 30 μmol h-1 g-1	λ> 420 nm (Xenon lamp, 300 W), pure water	Yes	Yes	***ACS Catal.*** 2016, 6, 7188−7196
4	Pt/$CuGaS_2$/RGO/$BiVO_4$/CoO_x	-	H_2: 35 μmol h^{-1} O_2: 17 μmol h^{-1}	λ> 420 nm (Xenon lamp, 300 W),	Yes	Yes	***J. Am. Chem. Soc.*** 2016, 138, 10260−10264
5	Ta_3N_5/$BaTaO_2N$	0.1% at 420 nm	H_2: 3.2 μmol h^{-1} O_2: 1.6 μmol h^{-1}	λ> 420 nm (300 W xenon lamp)	Yes	Yes	***Chem. Sci.***, 2017,**8**, 437-443
6	Ru loaded $SrTiO_3$:La, Rh/$BiVO_4$:Mo	19% at 419 nm	H_2: 3200 μmol h^{-1} g^{-1} O_2: 1600 μmol h-1 g-1	λ> 420 nm (300 W xenon lamp), pure water	Yes	Yes	***J. Am. Chem. Soc.*** 2017, 139, 1675−1683
7	RuO2/TiO2:Ta /N, Ru/$SrTiO_3$:Rh	0.5% at 420 nm	-	$NaIO_3$ or $FeCl_3$(1mM) solution	Yes	Yes	***J. Mater. Chem. A***, 2017,**5**, 18870-18877
8	MoS_2/CdS, Co_2O_3/$BiVO_4$	1.04% at 420 nm	H_2: 14.5 μmol h-1 O_2:7.1 μmol h-1	λ> 420 nm (300 W xenon lamp, output intensity of 200 mW/cm ^{2}),	Yes	No	***J. Mater. Chem. A***, 2017,**5**, 21205-21213
	Mediator and Co-Catalysts-Free Direct Z-scheme systems for Overall water splitting						
	Photocatalyst	**AQE**	**Activity**	**Conditions of photocatalytic reaction**	**Electrons Mediator**	**Co-Catalyst**	**Ref**
9	$Co_3(PO_4)_2$/α-Fe_2O_3	-	H_2: 0.63 μmol h^{-1} O_2: 0.32 μmol h^{-1}	400 nm < λ < 700 nm (LED),	**No**	**No**	***Catal. Sci. Technol.***, 2018,**8**, 840-

				Pure water			846
10	Bi_2WO_6-Cu_3P	-	H_2: 9.3 µmol/gcatalyst and 4.6 O_2:µmol/gcatalyst	AM 1.5G simulated sunlight with 100 mW cm^{-2}, Na_2HPO_4/ NaH_2PO_4 solution	**No**	**No**	***Nanoscale***, 2018,**10**, 3026-3036
11	$Si/MgTiO_2$	-	H_2: 159.33 µmol g^{-1} h^{-1}	>420 nm (Xenon lamp, 300 W), pure water	**No**	**No**	***Int. J. Hydrogen Energy***, 2016, **41**, 14713–14720
12	Black Phosphorus/$BiVO_4$	0.89% at 420 nm	H_2 :160 µmol g^{-1} h^{-1} O_2: 102 µmol g^{-1} h^{-1}	420 nm (Xenon lamp, 320W), Pure water	**No**	**No**	***Angew. Chem.*** *Int. Ed.* **2018**, *57*, 2160..
13	**Cs_2O-Bi_2O_3-ZnO**		**H_2 :149.5 µmol g^{-1} h^{-1}** **O_2: 73.2 µmol $g^{-1}h^{-1}$**	**AM 1.5G simulated sunlight with 100 mW cm^{-2}**	**No**	**No**	**The present work**

Table S4. Calculations of VBM and CBM from Tauc plot.

Semiconductor	**χ (eV)**	**Eg (eV)**	**CBM (eV)**	**VBM (eV)**
Cs_2O	3.89	1.96	-1.59	0.37
Bi_2O_3	5.99	2.74	0.12	2.86
ZnO	5.79	3.1	-0.26	2.84

Table S5. Calculations of VBM and CBM using VB-XPS analysis.

Semiconductor	**Eg (eV)**	**CBM (eV)**	**VBM (eV)**
Cs_2O	1.96	-1.55	0.41
Bi_2O_3	2.74	0.15	2.89
ZnO	3.10	-0.28	2.82

Table S6. Calculations of VBM and CBM from Mott-Schottky plots.

Semiconductor	**Eg (eV)**	**CBM (eV)**	**VBM (eV)**
Cs_2O	1.96	-1.52	0.44
Bi_2O_3	2.74	0.18	2.92
ZnO	3.1	-0.23	2.87

References

1 A. Band, A. Albu-Yaron, T. Livneh, H. Cohen, Y. Feldman, L. Shimon, R. Popovitz-Biro, V. Lyahovitskaya and R. Tenne, *J. Phys. Chem. B*, 2004, **108**, 12360–12367.

2 Y. Liu, Z. H. Kang, Z. H. Chen, I. Shafiq, J. a Zapien and I. Bello, *Cryst. Growth Des.*, 2009, **9**, 3222–3227.

3 S. Sood, A. Umar, S. Kumar Mehta and S. Kumar Kansal, *Ceram. Int.*, 2015, **41**, 3355–3364.

4 Y. C. Ma, Y. H. Guo, H. Y. Jiang, D. Qu, J. Liu, W. K. Kang, Y. Yi, W. Zhang, J. S. Shi and Z. Z. Han, New J. Chem., 2015, 39, 5612–5620.

5 A. Hezam, K. Namratha, Q. A. Drmosh, Z. H. Yamani and K. Byrappa, Ceram. Int., 2017, 43, 5292–5301.

6. G. Sadanandam, K. Lalitha, V. D. Kumari, M. V. Shankar and M. Subrahmanyam, *Int. J. Hydrogen Energy*, 2013, **38**, 9655–9664.